International Journal of Smart Home
Vol. 9, No. 5 (2015), pp. 73-82
http://dx.doi.org/10.14257/ijsh.2015.9.5.08

Rotary Shaft Structure Optimization of High-Temperature Motor Based on Ansys

Xi-fengWang[1,2], Da-weiMeng[1], and Yong-mingXu[1]

1 College of Electrical and Electronic Engineering, Harbin University of Science and Technology, Harbin 150080, China
2 College of Electrical and Electronic Engineering, Heilongjiang Institute of Technology, Harbin 150050, China
wangxiaoxu0104@163.com

Abstract

This thesis focuses on the problems of high-temperature furnace motor in term of rotary shaft over length as well as deformation tendency under high-temperature condition, and therefore the thesis conducts design optimization upon rotary shaft of a motor that is applied in high-temperature furnace regarding its mechanical property and thermal-stress distribution. First, it establishes a full-scale 3D model of the shaft-fan system, then it analyzes its mechanical properties such as rigidity and stiffness under the high-temperature environment, which bases on reasonable assumed conditions and the boundary conditions, where hence the thesis puts forwards an optimized dimension design solution for the motor rotary shaft. And then the thesis analyzes and calculates the shaft-fan system to improve the motor shaft size from the angle of thermal stress and thermal deformation consideration and the special characteristics of such motor working under high-temperature environment. And the improved motor shaft size is verified as reasonable. The thesis analysis can be the designing references for cooling system applied in the high-temperature furnace motor.

Keywords: *High-temperature furnace motor; rotary shaft-fan system; mechanical properties; size optimization*

1. Introduction

The application of small power motor technology in high-temperature furnace plays a significant role in the development and technical progress of the heat-treatment industry. The high-temperature furnace motor as the driving unit to the high-temperature treatment furnace fan, operates in very severe operation environment [1, 2]. Because the motor body is subject to extreme high furnace temperature and long cycle of operation as well as other influencing factors, and the motor rotary shaft has weak mechanical stability, therefore it tends to deform at the shaft extension side and in the fan impeller. If there is too much deformation at the shaft extension side, the rotary shaft would cause rotor core off its position, therefore the motor performance and reliability [3, 4] would be affected.

The literature [5] gives detailed analysis for the static and dynamic characteristics of motors in term of high-speed motors. It optimizes the structure of the motor shaft through theoretical calculation and FEM analysis but the operation condition under the high temperature is not considered. The literature [6] describes vibration influence to motors performance. And it optimizes dynamic characteristics of motor shafts by using multi-body transfer matrix method and FEM simulation. This thesis thoroughly analyzes the mechanical properties of a 4-pole and 22kW induction motor shaft and finalizes an optimum dimension design, and the overall study based on thermo-mechanical coupling FEM method, besides it takes reference to the dynamic characteristic research methods

ISSN: 1975-4094 IJSH

for the motor shaft from the literatures [5, 6] and takes the operation conditions under the high temperature (980°C) into consideration.

2. High-temperature Furnace Motors and Motor Rotary Shafts

At present Chinese heat treatment furnaces generally use sealed motors. Such motors have long rotary shafts design outside of the motor and motor flanges can directly connected to furnace covers. At the same time the motors use stainless steel seal cowlings between stators and rotors inside, which seal the rotor into the vacuum chamber and isolate it from the stator and outside housing. And at present the motors usually use static seal to replace the commonly used dynamic seal to improve technical performance. See Fig. 1 for high-temperature furnace sealed motor and its rotary shaft structure.

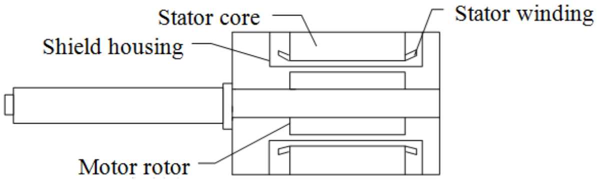

Figure 1. The Schematic Diagram of Furnace Motor

However in the recent years, the furnaces sealed motors frequently have problems [7] during operation, such as great deal of heat generated from the heat treatment furnace will be directly transferred onto the motor rotary shaft. Though the rotary shaft is made of selected high-resistant material, but the shaft extension would still deform under load if the main dimension of the shaft were unreasonable, especially when the motor operates under high-temperature environment. In worst case it may cause the stator scraps the rotor due to the rotor’s vibration. Therefore, researches on material properties selection, rigidity and strength analysis and calculation, static-mechanical characteristic studies, and thermal characteristic calculation for the furnace motor long shaft have become some of the hot topics home and abroad.

This thesis takes high-temperature and water cooling sealed motor for YRM series heat treatment furnace as example to optimize the rotary shaft design. The basic parameters of the motor are listed in table 1. In according to the actual situation it finds out that the motor heat transmission in axial direction is from left to right and from inside to outside in the radial direction. The heat transmission starts from the left shaft end to the front-cover cooling conduit through the rotary shaft. The cooling water will take away part of the heat, and the rest of the heat will continue move towards right direction to the motor stator. Both the motor stator and rotor will generate wear heat during operation, and such heat and the heat from the rotary shaft will conduct heat exchange with water jacket on the motor housing. The water jacket uses water cooling to cool off the rotor and stator. This is the heat transmission and cooling process of the water-cooling sealed motor for furnace.

Table 1. The Basic Parameters of the Studied Furnace Motor

Rated Power	2.2kW	OD of motor housing	217mm
Nominal Voltage	380V	cooling water pressure	≤0.5 Mpa
Rated Frequency	50Hz	Total length of motor	780mm
Rated Current	4.87A	cooling water flow rate	≥0.3m3/h
OD of rotor shaft D_1	38mm	Front bearing	18110
OD of shaft extension D_2	48mm	Rear bearing	M180206Z
Overhang length of rotary shaft L	430mm	Shaft-fan	Cr25Ni20

3. Mechanical Characteristic Study of Shaft-fan System

The overhang shaft of the high-temperature motor has to extend inside the heat treatment furnace to drive the fan, which requires the motor adopts special long shaft design. In former motor shaft design analysis, most of them only take the motor shaft as research subject, but only applying simple constraints and load can't simulate the working condition of the motor shaft in real environment. This thesis establishes a shaft-fan 3D model for high-temperature furnace motor with conventional rotary shaft designing method combining FEM technology, which is fully considered as the structural features of the high-temperature furnace motor and unique operation conditions. In this way, it avoids the inaccuracy exists with simulation calculation in separate parts and it can simulate the mechanical characteristic of the rotary shaft in more real working conditions.

The overall length of the subject motor shaft in the thesis is 980mm and the shaft overhang length is 430mm. The maximum furnace temperature can reach to about 980°C. The mechanical characteristics must be studied during the motor designing phase.

The motor shaft is supported by the front and rear bearings. And one end of the shaft is fixed and the other end is floating. The rear end of the shaft is fixed and the front end is floating which drives an external fan unit. In order to minimize the axial movement of the rotary shaft and improve the shaft stiffness, both the front and rear support bearings use deep-groove bearings. The established analysis and calculation model is shown in Fig. 2.

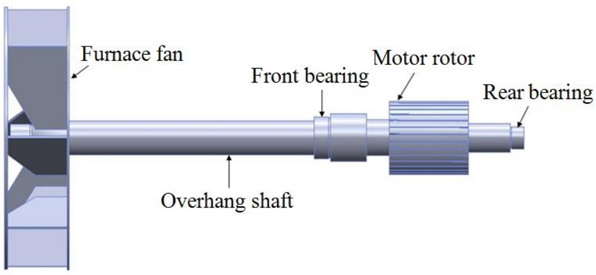

Figure 2. The Fan-shaft Calculation Model for Furnace Motor

First, the thesis analyses the rotary shaft's static characteristic, which is to learn the deformation and stiffness conditions of the shaft extension under the special operation situation and such analysis is significant to improving the motor's operation performance. It finds out through linear static structural analysis that force is not relevant to time, and therefore the displacement (x) calculation mathematical model can be expressed into the following matrix equation [8]:

$$[K]\{x\}=\{F\} \tag{1}$$

In which: $[K]$ is the rigidity factor matrix, (x) is the displacement vector and $\{F\}$ is force vector.

The motor rotary shaft is supported by the front and rear bearings. One shaft end is fixed and the other end is floating. The rear end of the rotary shaft is fixed, and the rear end of the shaft extension is floating. Model for the motor rotary shaft is shown in Fig. 3.

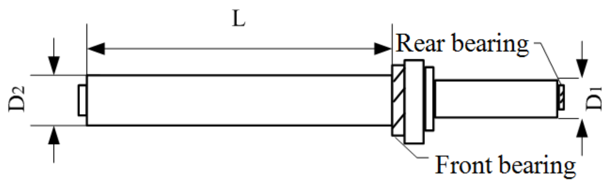

Figure 3. The Simplified Diagram of the Spindle Model

The 3D calculation analysis model for the motor centrifugal fan-shaft is built in correlation with the mathematical model. Besides, it gives corresponding constraints and load conditions. See Fig. 4. The main set constraints and loads are as below:

1)Simplify the bearings as flexible support at the cross between spindle axis and contact axis. Don’t consider the angular rigidity and axial rigidity of the bearings.

2)Apply constraints at A and B position on the cylinder surface shown in the Fig. 4. Apply 1900N and 750N radial force respectively on the bearings.

3)Apply 500N force at the motor rotor installation position in negative direction along Y-axis. The torque produced by the rotor distributes equally at the rotor installation position of the spindle unit. The torque value is 146900N/mm and along the negative direction of Z-axis.

4)Set the revolution speed for overall shaft-fan 1848 system at 24 rad/s around the negative direction of Z-axis.

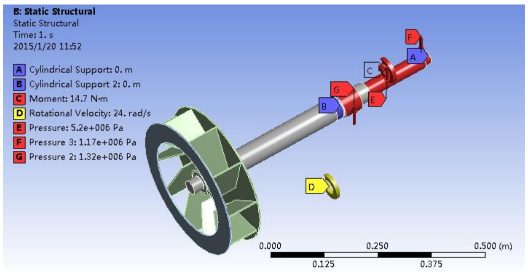

Figure 4. Constraint and Load of Main Fan System

Use FEM to conduct deformation and stress analysis and calculation on the centrifugal fan-shaft combined model. And it will get maximum deformation and equivalent stress distribution nephograms for the shaft-fan system, see Fig. 5 and 6.

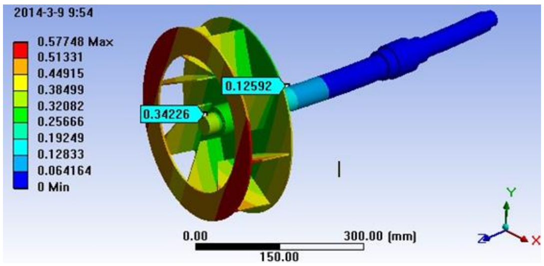

Figure 5. The Maximum Deformation Distribution

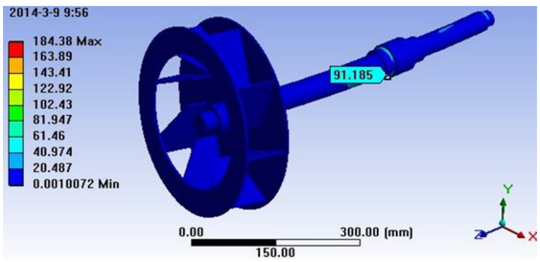

Figure 6. The Equivalent Stress Nephogram

It can find out from the maximum deformation nephogram in the Fig. 5 that the maximum deformation in the system appears in the front disk of the fan impeller at 0.57748m. And the maximum deformation of the spindle is 0.34mm exiting in the interface between the spindle and the fan. The maximum deformation at the near bearing end is 0.12mm. From Fig. 6 it can find out that the maximum equivalent stress 91MPa appears on the overhang shaft where the spindle diameter changes at the near bearing side.

4. Shaft-fan System Improvement based on the Mechanical Characteristics

The motor rotary shaft transfers torque and bears the bending moment at the same time. Properly increase the shaft diameter can improve its mechanical performance. This thesis focus on the over length of the overhang shaft and proposes an optimized design for the shaft diameter and shaft overhang length.

From the above analysis in the Fig. 6 it can find out the fan deforms a lot and the rotary shaft bends when the shaft extension diameter is of 48mm and the shaft overhang is 430mm long. The design optimization towards the rotary shaft diameter and the overhang length is to ensure permissible deformation and stress under normal condition and high-temperature situation. Define the rotary shaft overhang length as L, and define the shaft extension diameter D_2 as parametric variable, which is set between 40-60mm. And set the shaft extension L which is at the motor front bearing side between 400-450mm. The target is to find out an optimum solution between the shaft deformation and the shaft extension length. Through calculation the relation among the rotary shaft diameter, the shaft extension length and the total deformation are obtained, see Fig.7 and 8.

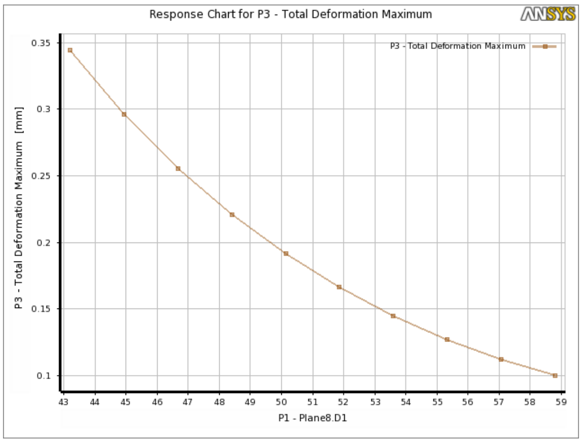

Figure 7. The Relationship between Amount of Deformation and Shaft Diameter

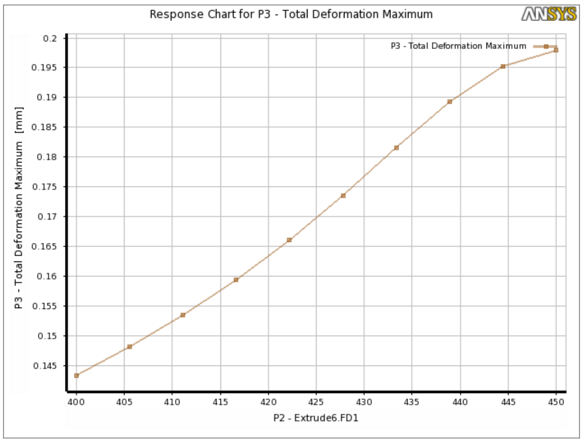

Figure 8. Shaft Extension Length and Deformation Relations

The shaft deformation decreases as the shaft diameter increases and the deformation increases when the shaft extension length increases.

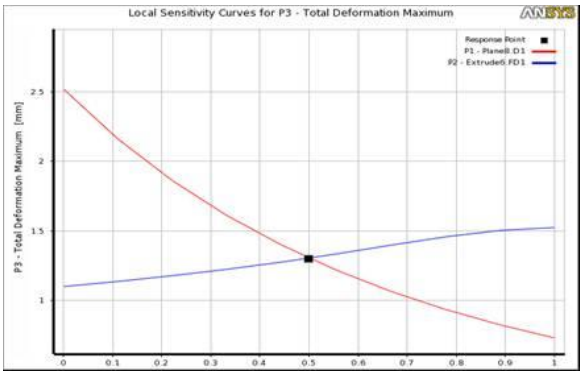

Figure 9. The Diameter of the Main Shaft and the Shaft Overhang Optimal Solution

It can find out from the Fig. 9 that the optimum solution is when the shaft diameter is 55mm and the shaft overhang length is 422mm. The total deformation status of the rotary shaft in the optimum solution is shown in Fig. 10 and the equivalent stress nephogram is shown in Fig. 11.

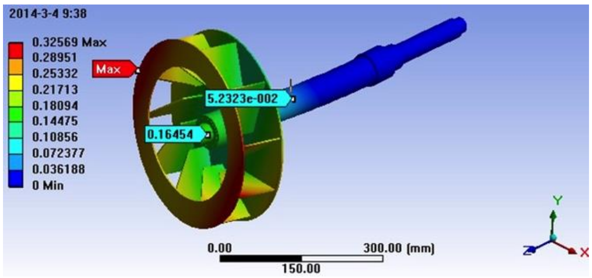

Figure 10. The Total Deformation of 55mm Spindle

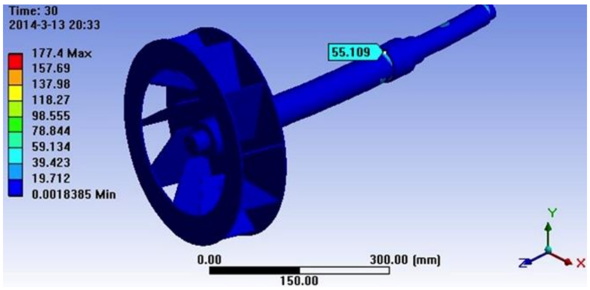

Figure 11. The Equivalent Stress Nephogram of 55mm Spindle

Front Fig. 10 it can find out that after the shaft structure is optimized, the maximum deformation in the shaft-fan system still exists in the front disk of the fan and the maximum displacement at the moment is 0.325mm. The maximum deformation in the shaft exists where the shaft connects to the fan, which is near the fan side with about 0.16 displacements. From the Fig. 11, at this time the maximum equivalent stress in the shaft front bearing side is 55MPa. In the motor shaft-fan system, diameter-55 shaft can meet the requirements for the first and fourth strength level and compare the Fig. 5 with Fig. 6, the deformation status of the diameter-55mm shaft is better than that of the diameter-

48mm shaft, and its stress and strain are both less than the maximum permissible deformation value stated in the national standard. Therefore, 55mm-diameter shaft-fan system fully fulfills the stiffness and rigidity requirements.

5. Rotary Shaft-fan System Optimization based on Thermal-mechanical Characteristic

The rotary shaft-fan is the main heat transmission unit for the high-temperature sealed furnace motor. The main heat source is the high-temperature gas inside the sealed furnace. The high temperature gas will cause thermal deformation, which will influence the stability of the rotary shaft-fan system. Such high temperature not only limits the rigidity level for the motor shaft, but also limits the operation performance and service life [9] of a furnace motor. Hence, it must conduct thermal characteristic analysis upon the shaft-fan system during the designing phase.

The sample motor in this thesis uses heat exchange mode as heat transmission, which is transferring the furnace internal heat to outside through the shaft-fan system. And compare with the heat from the heat-treatment furnace, the motor wear heat and bearing friction heat can be ignored. During the thermal analysis, use the following boundary conditions and load conditions in the shaft-fan simulation model:

1)Ambient temperature is 22°C

2) The revolution speed of the shaft-fan system is 1420r/min

3) Ignore the heat comes from bearing friction or between the stator and the rotor

4)Consider the operation environment of the motor, and ignore the air convection and radiation between the shield housing, rotor, motor housing and the ambient air.

5)Take temperature as load and apply it onto the shaft.

6)The starting temperature is 980°C.

Based on the above mentioned heat transmission differential equation and the boundary conditions, it can get boundary value problems of steady temperature field for an anisotropic medium model [10][11]

$$\left.\begin{array}{l} \dfrac{\partial}{\partial x}(\lambda_x \dfrac{\partial T}{\partial x}) + \dfrac{\partial}{\partial y}(\lambda_y \dfrac{\partial T}{\partial y}) + \dfrac{\partial}{\partial z}(\lambda_y \dfrac{\partial T}{\partial z}) = -q_V \\ \lambda \left.\dfrac{\partial T}{\partial n}\right|_{s_2} = q_0 \\ \lambda \left.\dfrac{\partial T}{\partial n}\right|_{s_3} = -\alpha(T - T_f) \end{array}\right\} \tag{2}$$

In which: T is temperature, λ_x, λ_y and λ_z are anisotropic heat conductivity coefficient, T_f is temperature of the ambient medium, α is heat exchange coefficient among the ambient medium.

If the distribution function of the T is known, it can apply numerical integration into the above equation to get results. Especially when T is a polynominal expression for x and y, then it is easier to write accurate integral expression. In this case, the equivalent nodal load matrix for thermal stress is:

$$\{H\}^e = \frac{E\alpha(T_i + T_j + T_m)t}{6(1-\mu)}\begin{bmatrix} b_i & c_i & b_j & c_j & b_m & c_m \end{bmatrix}^T \tag{3}$$

In which: T_i, T_j and T_m are respective temperatures at nodes i, j and m.

Fig. 12 is obtained through calculation. It is a temperature nephogram of different diameter rotary shafts under the same temperature and heat conductivity coefficient. From the temperature nephogram, it shows the size of shaft diameter influence the size of heat resistance and heat transmission path. The heat conduction of the 55mm shaft is lower than that of the 48mm shaft. For 55mm-diameter shaft, the temperature at the front shaft bearing is 216.73°C. And for 48mm-diameter shaft, the temperature at the front shaft bearing is 469.32°C. The overall shaft temperature reduces from the fan side toward the bearing side. The furnace motor uses high-temperature resistant bearing, which in some level prevents the heat conduction. If motors work under such conditions for long cycle, it will cause inevitable damage to the motors and thus reduces the service life.

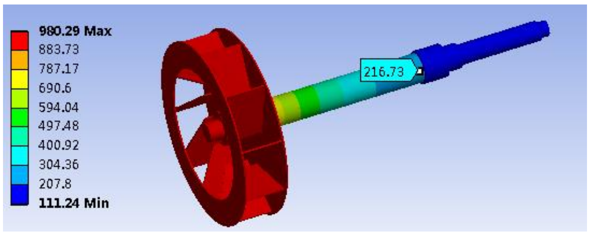

a) Temperature Distribution Nephogram for 55mm Shaft

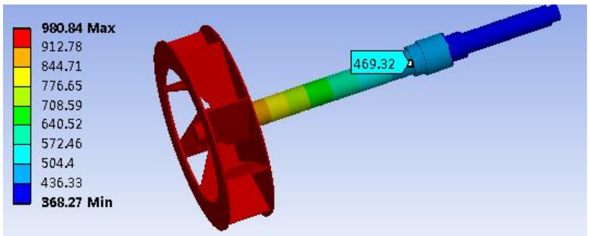

b) Temperature Distribution Nephogram for 48mm Shaft

Figure 12. Temperature Distribution in Spindle

By use of FEM analysis method and use the actual temperature distribution that is transferred to the front bearing temperature field as thermal load, then apply it to the static-mechanical structural model for coupled thermo-mechanical analysis and then it can calculate thermal stress and strain results of the shaft-fan system. Fig. 13 is an equivalent stress nephogram from coupled thermo-mechanical analysis, which uses temperature as load condition. From the Figure it can find out that the maximum equivalent stress for 55mm shaft-fan system is 320.91MPa, and the front shaft bearing has 108.75MPa equivalent stress. And the maximum equivalent stress for 48mm shaft-fan system is 527.01MPa in the shaft extension where is close to the front shaft bearing. Equivalent stress distribution at the motor stator position is larger than that of the 55mm-diameter shaft, which is 282.93 MPa, and the value exceeds the material stress strength value (205 MPa).

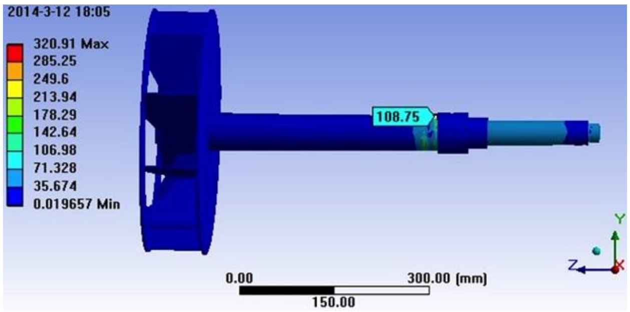

a) Equivalent Stress Nephogram for 55mm Shaft

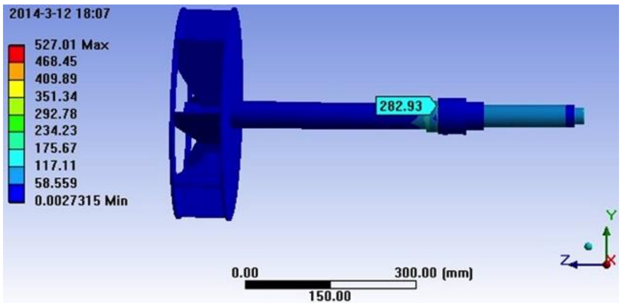

b) Equivalent Stress Nephogram for 48mm Shaft

Figure 13. Temperature distribution in spindle

Fig. 14 is a calculated nephogram for the total system deformation, which uses temperature as load condition for coupled thermo-mechanical analysis.

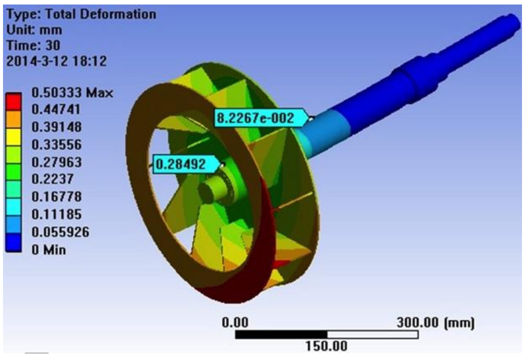

a) Total Deformation Nephogram for 55mm Shaft

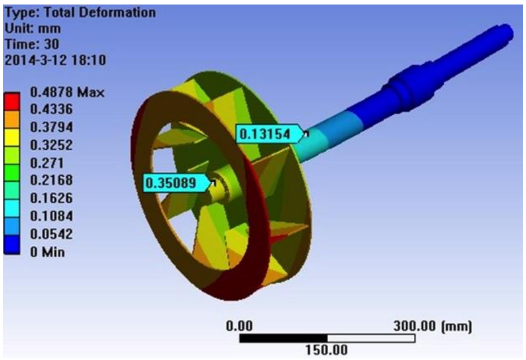

b) Total Deformation Nephogram for 48 mm Shaft

Figure 13. The Total Deformation of Spindle

It can find out from the above Figure that the maximum equivalent strain for 55mm shaft-fan system is 0.5mm. The maximum deformation exists in the front fan disk and the maximum deformation in the shaft is 0.28mm. And the maximum equivalent strain for 48mm shaft-fan system is 0.48mm and the maximum deformation exists in the front fan disk with 0.35mm maximum deformation in the shaft. It can also find out from the Figure that the shaft strain of 48mm motor is larger than that of the 55mm motor. The optimized rotary shaft has improved working performance.

6. Conclusion

This thesis establishes an integrated 3D full-scale model of the shaft-fan system and adds proper constrains and load conditions in reference to the actual working conditions, and the thesis analyzes the static-mechanical characteristic of the rotary shaft-fan system in term of deformation and equivalent stress. Also the thesis uses mechanical designing theories in combining with FEM optimization principle to conduct parametric setting to diameter size and shaft overhang length of the shaft unit, through which it verifies the optimum sizes and the performance is improved dramatically after the optimization. And then, the thesis gives coupled thermal-mechanical analysis to the shaft-fan system to determine the boundary conditions for thermo-mechanical coupling, in this way it obtains the systematic temperature distribution, equivalent stress values and total deformation values. In addition, the thesis analyzes the furnace temperature influence in regard of the system deformation and stress, and it proves the optimized shaft has better thermal features. All the analysis and calculation conducted in this thesis can be used as theoretical references for designing cooling system of the high-temperature furnace motor.

References

[1] Z. X. Li, Z. W. Sun, G. J. Yao and G. J. Sun, "Application and Structure Features of Furnace Sealed Motor", Industrial Heating, no. 1, **(2000)**, pp. 47-49.
[2] P. Xue and J. W. Zhu, "A Study of the Jacking System for Furnace Electrode Based on Linear Motor", The Ninth International Conference on Electronic Measurement and Instruments, **(2009)**; China.
[3] X. Chen and J. F. Liu, "Thermal Properties and Influence of High-Speed Spindle", Journal of Mechanical Engineering, vol. 49, no. 11, **(2013)**, pp. 135-141.
[4] X. D. Yu, Q. H. Zhou, Z. Q. Wang, D. Liu, X. Fu, L. Tan, H. H. Li, "Velocity Performance of Temperature Field of High Speed and High Load Hydrostatic Thrust Bearing", Journal of Harbin University of Science and Technology, vol. 1, **(2014)**, pp. 1-4.
[5] C. Kang, "Study of Structural Design and Performance of High-Speed Electrical Spindle", Xi'an, Shaanxi University of Science & Technology, **(2013)**.
[6] K. Huang and Z. X. Zhang, "Dynamic Performance Modeling and Simulation of Electric Spindle System based on HyperMesh", Journal of System Simulation, vol. 25, no. 6, **(2013)**, pp. 1393-1398.
[7] Z. X. Li, "Application and Structure Features of Furnace Sealed Motor", Industrial Heating, no. 1, **(2000)**, pp. 47-48.
[8] S. M. Ma and Y. L. Ke, "FEM Analysis on Static-Dynamic Properties of High Efficiency Permanent Magnetic Synchronous Motor Shaft Based on ANSYS", Journal of Machine Design, vol. 30, no. 2, **(2013)**, pp. 82-85.
[9] C. H. Zeng and H. P. Liao, "Motor Shaft Structure and Optimization", Mechanical and Electrical Equipment, no. 2, **(2005)**, pp. 43-45
[10] W. L. Li, T. T. Chen and F. B. Qu, "Analysis of Solid Rotor 3D Temperature Field of High Efficiency Permanent Magnetic Synchronous Motor", Proceedings of the CSEE, vol. 30, no. 18, **(2001)**, pp. 55-60.
[11] H. Y. Wang, P. S. Su and X. H. Wang, "Calculation on the thermal field of the water cooling stator of three-Gorge hydrogernerator", Proceedings of the eighth International Conference on Electrical Machines and Systems, **(2005)**;Nanjing, China.

